SURFACE TREATMENT OF THE PROTOTYPE SPOKE CAVITY FOR THE JAEA-ADS LINAC*

J. Tamura†,1, T. Dohmae[2], Y. Fuwa[1], E. Kako[2], J. Kamiya[1], Y. Kondo[1], S. Kurosawa[1], F. Maekawa[1], S. Meigo[1], H. Sakai[2], K. Umemori[2], I. Yamada[1], B. Yee-Rendon[1]
[1]J-PARC, JAEA, Ibaraki, Japan
[2]iCASA, KEK, Ibaraki, Japan

Abstract

Japan Atomic Energy Agency (JAEA) has been proposing an accelerator-driven nuclear transmutation system (ADS). As a first step toward the practical design of the JAEA-ADS linac, we have been prototyping a low-β ($\approx$0.2) single-spoke cavity. Fabrication of the prototype spoke cavity was finally completed in FY2024. We are currently working on surface preparation for a high-field cavity testing at liquid helium temperature. In FY2025, we performed chemical polishing on the inner surface of the fabricated cavity, and subsequently proceeded to vacuum heat treatment. Although a uniform removal of the surface layer could not be achieved as initially anticipated, there were no defects observed on the inner surface. Hydrogen content of the chemically polished cavity was reduced through the furnace baking at J-PARC.

INTRODUCTION

JAEA has been proposing an ADS as a future nuclear system to efficiently reduce high-level radioactive waste generated in nuclear power plants. In the JAEA-ADS, a high-power proton beam of 30 MW with a final energy of 1.5 GeV is required with high reliability. The latest design of the JAEA-ADS linac is reported in Refs. [1,2]. As shown in Fig. 1, the proposed linac consists of a radio-frequency quadrupole (RFQ), half-wave resonator (HWR), low-β and high-β single-spoke resonators (SSR1 and SSR2, respectively), and low-β and high-β elliptical cavities (ELL1 and ELL2, respectively).

Figure 1: Proposed acceleration structure of the JAEA-ADS linac.

As a first step toward the practical design of the JAEA-ADS linac, we have been prototyping the low-β ($\approx$0.2) single-spoke cavity. The prototype spoke cavity with an operating frequency of 324 MHz was designed by electromagnetic simulation [3], and its dimensional parameters were optimized for higher cavity performance [4, 5]. Figure 2 shows the cross-sectional views of the designed cavity with surface electric and magnetic field distributions. The cavity's design parameters are listed in Table 1.

* This work was supported by JSPS KAKENHI Grant Number JP24H00235.
† jtamura@post.j-parc.jp

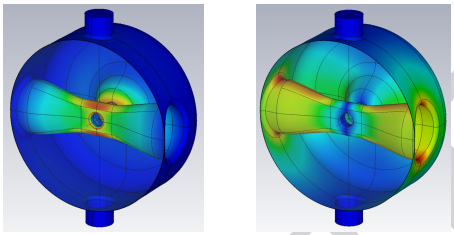

Figure 2: Cross-sectional views of the designed cavity with surface electric (left) and magnetic (right) field distributions.

Table 1: Design Parameters of the Prototype Spoke Cavity

Parameter	Value
f_0	324 MHz
β_g	0.188
β_{opt}	0.24
Beam aperture	40 mm
Cavity diameter	498 mm
Cavity length	300 mm
$L_{eff} = \beta_{opt}\lambda$	222 mm
$G = Q_0 R_s$	90 Ω
$T(\beta_{opt}) = V_{acc}/V_0$	0.81
$r/Q = V_{acc}^2/\omega U$	240 Ω
E_{peak}/E_{acc}	4.1
B_{peak}/E_{acc}	7.1 mT/(MV/m)

The actual cavity fabrication started in FY2020 and continued through the end of FY2024 [6–10]. The prototype spoke cavity is made of pure niobium (Nb), except for the niobium-titanium alloy (Nb-Ti) flanges for the RF ports and beam ports. The major parts were press-formed from 3.5 mm-thick Nb sheets. The nose-shaped end drift-tubes and the port flanges were machined from Nb and Nb-Ti cylindrical blocks, respectively. The shaped cavity parts were joined together by electron-beam welding (EBW), and the EBW assembly of the cavity without helium jacket was finally completed in FY2024.

We are currently proceeding with surface preparation for a high-field cavity testing at liquid helium temperature. In this paper, surface treatment processed to the prototype spoke cavity in FY2025 is presented.

CHEMICAL POLISHING

The inner surface of the fabricated spoke cavity was chemically polished with buffered chemical polishing (BCP) process so that the cavity may achieve sufficiently high field gradient. The BCP acid mixture of nitric acid (67.5 %), hy-

drofluoric acid (55 %), and phosphoric acid (85 %) was used in a volume ratio of HNO_3 : HF : H_3PO_4 = 1 : 1 : 3. During the BCP, the cavity was positioned with the RF ports along the vertical axis and the beam ports along the horizontal axis as shown in Fig. 3. The BCP fluid enters the cavity through the bottom RF port and the horizontal beam ports, and then, exits through the top RF port. In order to prevent air bubbles or reaction gas (nitrogen oxide) accumulating on the top surface inside the beam pipes, a similar amount of the BCP fluid was introduced through the two beam ports in total as was introduced through the bottom RF port. The BCP was performed in two separate sessions by flipping the cavity upside down to ensure symmetry in the removal amount of Nb surface layer. For this bulk BCP, we aimed to remove approximately 75 µm of the surface layer in a single session, with a total removal target of 150 µm as in [11, 12]. Before and after the bulk BCP, inside the cavity was ultrasonic-cleaned with pure water.

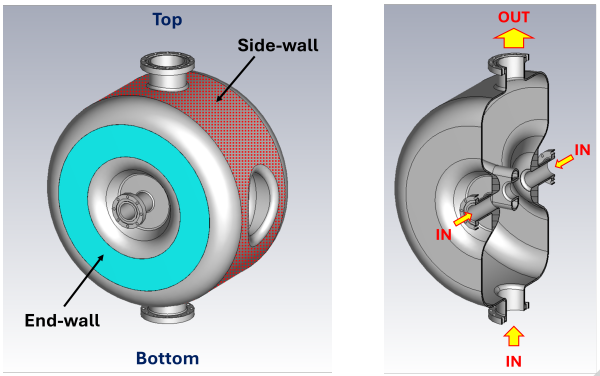

Figure 3: [Left] Directional configuration of the cavity during the BCP. [Right] Inlet and outlet of the BCP fluid.

In this bulk BCP, a uniform removal of the surface layer could not be achieved as initially anticipated. During the BCP, reduction in wall thickness was periodically measured using an ultrasonic thickness gauge. In the first session of the bulk BCP, we measured only the end-wall thickness as a reference of the polishing progress. When the thickness reduction in the end-walls reached 50-85 µm, we measured upper side-wall thickness and found that approximately 200 µm of the inner surface layer had been already removed. Therefore, we decided to terminate the first bulk BCP session to prevent excessive polishing. The thickness measurement after the first session revealed that the upper side-wall had been significantly more polished than the lower side-wall, with the surface layer removal of approximately 250 µm in upper and 50 µm in lower. In the second session of the bulk BCP where the cavity was inverted vertically relative to the first session, we prioritized ensuring a symmetrical distribution of the thickness reduction rather than focusing on achieving the initially targeted polishing amount. Consequently, we processed roughly the same amount of surface layer removal as in the first bulk BCP session.

The total amount of surface layer removal with this bulk BCP was 115-155 µm in the end-walls and 300 µm in the side-wall. In each bulk BCP session, due to the chemical reaction heat, temperature of the cavity and circulating BCP fluid eventually exceeded 25°C and 20°C, respectively. It was recognized that we should increase the cooling capacity of the BCP system, while it is unclear to what extent the insufficient cooling affected the uniformity of the surface layer removal. Adjusting the flow rate of the BCP fluid introduced through each port may help improve the polishing uniformity, as the removal rate is strongly correlated to fluid velocity [13]. However, it should be noted that, due to the complexity of the internal structure of the spoke cavity, it is difficult to achieve a uniform fluid velocity entirely on the cavity's inner surface. Therefore, in the future, a rotational BCP [12] is considered to be desirable rather than the stationary BCP.

It was confirmed after the bulk BCP by visual inspection that the inner surface of the cavity was polished to mirror-like finish and there were no defects such as air pocket or bubble striking. Figure 4 shows the inside view of the cavity as seen through the RF port. We measured the cavity's resonance frequency after the bulk BCP. The measured frequency was 324.27 MHz, which was converted to 324.37 MHz in vacuum taking into account the permittivity effect. It was found that the frequency was increased by 0.47 MHz compared to before the bulk BCP. According to the electromagnetic simulation [3], it was implied that thickness reduction in spoke electrode and/or EDTs, which are difficult to measure using an ultrasonic thickness gauge, is much larger than that in the side-wall.

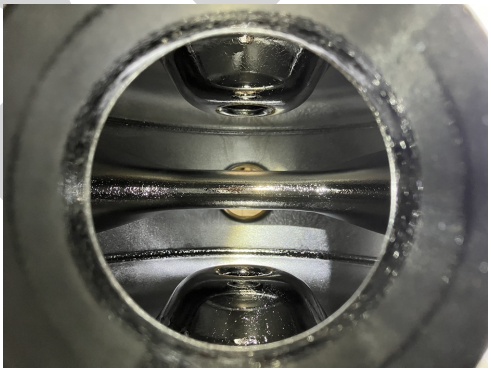

Figure 4: Inside view of the cavity, which has been processed with the bulk BCP, as seen through the RF port.

HEAT TREATMENT

For hydrogen degassing, the cavity processed with the bulk BCP was heat-treated at 600°C for 10 hours in the J-PARC vacuum furnace. Treating cavities at higher temperatures (for example, 800°C often applied to 1.3 GHz elliptical cavities) would reduce considerably the plateau time. The prototype spoke cavity is not jacketed with helium tank and there are no brazing joints of copper or stainless steel. In addition, spoke cavities, in which both ends of the spoke are terminated to the outer conductor, are considered to be structurally robust compared to quarter-wave resonators. Therefore, temperatures higher than 600°C may be applica-

ble. However, as the first campaign of the surface preparation for the cold testing, we followed the standard recipe of the community [11, 14]. Provided that sufficient annealing time is ensured, a temperature of 600°C would not be too low for desorbing hydrogen from chemically polished Nb material [15]. Figure 5 shows the prototype spoke cavity installed in the J-PARC vacuum furnace. The oil-free vacuum furnace was evacuated by three turbomolecular pumps (each with a pumping speed of 3200 L/s) with a dry scroll pump as the fore-pump. During the heat treatment, there were no Nb caps equipped on any of the cavity ports.

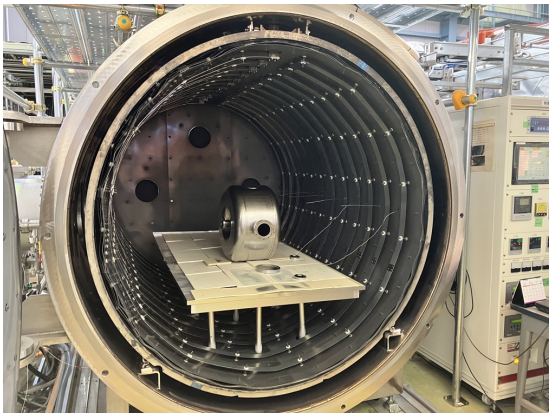

Figure 5: Prototype spoke cavity installed in the J-PARC vacuum furnace.

It was confirmed by residual gas analysis that hydrogen was the predominant desorbed gas component during the heat treatment. In this furnace baking, temperature was slowly raised from room temperature to 600°C at a rate of +100°C per hour. After keeping the temperature at 600°C for 10 hours, it was lowered to around 400°C at a rate of -100°C per hour. And then, heater output was turned off, and the system was switched to natural cooling. Figure 6 shows the total pressure variation in response to the applied temperature. While the temperature was kept at 600°C, the most significantly desorbed gas was hydrogen. Furthermore, based on the preliminary trial using the same temperature pattern but without placing the cavity in the furnace, there was no significant difference in each ion current, with the exception of hydrogen, between cases with and without the cavity inside the furnace. Figure 7 shows the variations in the ion current of H_2 and H_2O measured using quadrupole mass spectrometer. Since the decrease in hydrogen ion current has not yet saturated even at the end of the 10-hour plateau period, extending the annealing period at 600°C would likely result in further hydrogen degassing.

There was no change in resonance frequency of the cavity before and after the heat treatment. Therefore, it is likely that no deformation of the cavity shape occurred as a result of the heat treatment. As the next surface processing, this heat treatment is supposed to be followed by light BCP to remove a few tens of microns of the inner surface which might be polluted by the residual gas re-absorbed at the end of the process.

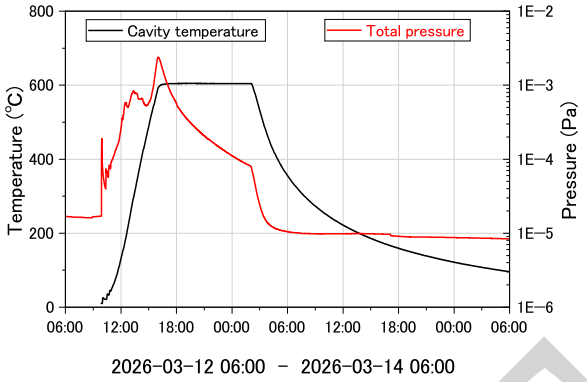

Figure 6: Temperature dependence of the total pressure in the vacuum furnace during the heat treatment.

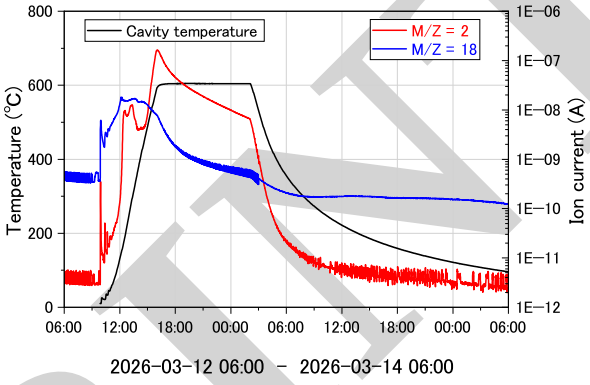

Figure 7: Temperature dependence of the ion current of H_2 (red) and H_2O (blue) during the heat treatment.

CONCLUSION

We performed the bulk BCP on the inner surface of the fabricated spoke cavity so that the cavity may achieve sufficiently high field gradient. Subsequently, we annealed the cavity for hydrogen degassing at 600°C for 10 hours in the J-PARC vacuum furnace. In preparation for the cold test, we are proceeding to the next surface treatment such as light BCP and high-pressure cavity rinsing with ultra-pure water.

ACKNOWLEDGEMENTS

We would like to thank the staff of MARUI GALVANIZING Co., Ltd. for processing the bulk BCP and ultrasonic cleaning to the prototype spoke cavity.

REFERENCES

[1] B. Yee-Rendon, Y. Kondo, F. Maekawa, S. Meigo, and J. Tamura, "Design and Beam Dynamic Studies of a 30-MW Superconducting Linac for an Accelerator-Driven Subcritical System", *Phys. Rev. Accel. Beams*, vol. 24, p. 120101, 2021. doi:10.1103/PhysRevAccelBeams.24.120101

[2] B. Yee-Rendon, Y. Kondo, J. Tamura, K. Nakano, F. Maekawa, and S. Meigo, "Beam Dynamics Studies for Fast Beam Trip Recovery of the Japan Atomic Energy Agency Accelerator-Driven Subcritical System", *Phys. Rev. Accel. Beams*, vol. 25, p. 080101, 2022.

doi:10.1103/PhysRevAccelBeams.25.080101

[3] CST Studio Suite, https://www.3ds.com/products/simulia/cst-studio-suite

[4] J. Tamura *et al.*, "Electromagnetic Design of the Prototype Spoke Cavity for the JAEA-ADS Linac", in *Proc. SRF'19*, Dresden, Germany, Jun.-Jul. 2019, pp. 399–402. doi:10.18429/JACoW-SRF2019-TUP007

[5] J. Tamura *et al.*, "RF Design of the Prototype Spoke Cavity for the JAEA-ADS Linac", in *Proc. 3rd J-PARC Symposium (J-PARC'19)*, Tsukuba, Japan, vol. 33, p. 011049, 2021. doi:10.7566/JPSCP.33.011049

[6] J. Tamura *et al.*, "Present Status of the Spoke Cavity Prototyping for the JAEA-ADS Linac", in *Proc. SRF'21*, East Lansing, MI, USA, Jun.-Jul. 2021, pp. 612–615. doi:10.18429/JACoW-SRF2021-WEPCAV011

[7] J. Tamura *et al.*, "Current Status of the Spoke Cavity Prototyping for the JAEA-ADS Linac", in *Proc. LINAC'22*, Liverpool, UK, Aug.-Sep. 2022, pp. 180–183. doi:10.18429/JACoW-LINAC2022-MOPOGE14

[8] J. Tamura *et al.*, "Fabrication progress of the prototype spoke cavity for the JAEA-ADS linac", in *Proc. IPAC'23*, Venice, Italy, May 2023, pp. 1588–1590. doi:10.18429/JACoW-IPAC2023-TUPA120

[9] J. Tamura *et al.*, "Progress of the spoke cavity prototyping for the JAEA-ADS linac", in *Proc. LINAC'24*, Chicago, IL, USA, Aug. 2024, pp. 496–498. doi:10.18429/JACoW-LINAC2024-TUPB078

[10] J. Tamura *et al.*, "Fabrication of the prototype spoke cavity for the JAEA-ADS linac", in *Proc. SRF'25*, Tokyo, Japan, Sep. 2025, paper THP39, pp. 691–694.

[11] L. Ristori *et al.*, "Cold Tests of SSR1 Resonators Manufactured by IUAC for the Fermilab PIP-II Project", in *Proc. SRF'15*, Whistler, Canada, Sep. 2015, pp. 750–753. doi:10.18429/JACoW-SRF2015-TUPB073

[12] M. Moretti, Y. N. Hoerstensmeyer, F. Marhauser, and A. Navitski, "Fabrication and Surface Treatment of Superconducting Rf Single Spoke Cavities for the Myrrha Project", in *Proc. SRF'23*, Grand Rapids, MI, USA, Jun. 2023, pp. 578–583. doi:10.18429/JACoW-SRF2023-TUPTB067

[13] F. Éozénou *et al.*, "Investigation of BCP Parameters for Mastery of SRF Cavity Treatment", in *Proc. SRF'17*, Lanzhou, China, Jul. 2017, pp. 558–562. doi:10.18429/JACoW-SRF2017-TUPB072

[14] D. Longuevergne, "Review of Heat Treatments for Low Beta Cavities : What's So Different from Elliptical Cavities", in *Proc. SRF'17*, Lanzhou, China, Jan. 2018, pp. 708–714. doi:10.18429/JACoW-SRF2017-THXA08

[15] J. Kamiya *et al.*, "Investigation of Niobium Surface Roughness and Hydrogen Content with Different Polishing Conditions for Performance Recovery of Superconducting QWRs in JAEA Tokai-Tandem Accelerator", *e-J. Surf. Sci. Nanotechnol.*, vo. 21, no. 4, pp. 344–349, 2023. doi:10.1380/ejssnt.2023-046